In vitro models (2022) 1:241–247
https://doi.org/10.1007/s44164-022-00022-z

RAPID COMMUNICATIONS

A novel colorimetric biosensor for detecting SARS-CoV-2 by utilizing the interaction between nucleocapsid antibody and spike proteins

Abhishek Bhattacharjee[1] · Roberta M. Sabino[1] · Justin Gangwish[1] · Vignesh K. Manivasagam[2] · Susan James[1,2,3] · Ketul C. Popat[1,2,3] · Melissa Reynolds[3,4,5] · Yan Vivian Li[1,3,6]

Received: 8 April 2022 / Revised: 17 May 2022 / Accepted: 18 May 2022 / Published online: 1 June 2022

Abstract

SARS-CoV-2 is a pandemic coronavirus that causes severe respiratory disease (COVID-19) in humans and is responsible for millions of deaths around the world since early 2020. The virus affects the human respiratory cells through its spike (S) proteins located at the outer shell. To monitor the rapid spreading of SARS-CoV-2 and to reduce the deaths from the COVID-19, early detection of SARS-CoV-2 is of utmost necessity. This report describes a flexible colorimetric biosensor capable of detecting the S protein of SARS-CoV-2. The colorimetric biosensor is made of polyurethane (PU)-polydiacetylene (PDA) nanofiber composite that was chemically functionalized to create a binding site for the receptor molecule—nucleocapsid antibody (anti-N) protein of SARS-CoV-2. After the anti-N protein conjugation to the functionalized PDA fibers, the PU-PDA-NHS-anti fiber was able to detect the S protein of SARS-CoV-2 at room temperature via a colorimetric transition from blue to red. The PU-PDA nanofiber-based biosensors are flexible and lightweight and do not require a power supply such as a battery when the colorimetric detection to S protein occurs, suggesting a sensing platform of wearable devices and personal protective equipment such as face masks and medical gowns for real-time monitoring of virus contraction and contamination. The wearable biosensors could significantly power mass surveillance technologies to fight against the COVID-19 pandemic.

Keywords SARS-CoV-2 · COVID-19 · Biosensor · Polydiacetylene · Nanofiber

Several coronaviruses from the family of *Coronaviridae* used to cause mild respiratory diseases until the severe acute respiratory syndrome coronavirus (SARS-CoV) was transmitted from animal to human and caused the severe acute respiratory syndrome (SARS) disease in 2002 [1]. In December 2019, a cluster of patients with severe respiratory syndrome (pneumonia) was reported in Wuhan, China, and the associated pathogen was identified as a novel coronavirus [2], which was later named as SARS-CoV-2, and the disease was named as COVID-19. Since then, the COVID-19 cases have been reported in every continent including Antarctica. On 11 March 2020, the World Health Organization (WHO) declared the COVID-19 as a pandemic [3]. As of 15 November 2021, the total number of COVID-19 cases reported by WHO is more than 252 million with an associated death of more than 5 million individuals [4]. This novel coronavirus is the seventh edition in the *Coronaviridae* family of viruses that causes respiratory diseases in humans. The spreading capability of the new virus (SARS-CoV-2) is higher than all the other coronaviruses and new variants of SARS-CoV-2 spread even faster in humans than the original virus. SARS-CoV-2 has glycosylated spike (S) proteins [5] that binds to the angiotensin-converting enzyme II (ACE2) receptor found in lower respiratory tracts of humans [6]. The virus can survive on plastic, metal, or cardboard surfaces for 4 h up to 3 days, making it easier for the virus to spread [7]. To minimize the rapid spread of SARS-CoV-2,

✉ Yan Vivian Li
yan.li@colostate.edu

1 School of Advanced Materials Discovery, Colorado State University, Fort Collins, CO, USA

2 Department of Mechanical Engineering, Colorado State University, Fort Collins, CO, USA

3 School of Biomedical Engineering, Colorado State University, Fort Collins, CO, USA

4 Department of Chemistry, Colorado State University, Fort Collins, CO, USA

5 Department of Chemical and Biological Engineering, Colorado State University, Fort Collins, CO, USA

6 Department of Design and Merchandising, Colorado State University, Fort Collins, CO, USA

effective viral detection methods are necessary. The most popular method of SARS-CoV-2 detection is the real-time reverse transcription-polymerase chain reaction (rRT-PCR). However, it has several limitations such as complex protocols, the need for trained personnel, long turnaround, and false-negative results [8]. Different detection techniques have been developed since 2019 including plasmonic-based colorimetric assays, antibody capture, and antigen-binding assays, paper-based biomolecular sensors, and thermoplasmonic chips [9]. However, there is still a need to develop effective, highly selective, and easy-to-use detection methods for SARS-CoV-2.

Recently, polymeric materials such as polydiacetylene (PDA) that have colorimetric responses to environmental stimuli have gained great interest in developing colorimetric biosensors [10–14]. Previous studies suggested that PDAs have demonstrated colorimetric transition responses to various bacteria and viruses [11, 15]. Charych et al. (1993) first reported a PDA-based sensor that could detect hemagglutinin of the influenza virus [16]. Lately, PDA-based sensors have been reported to detect influenza virus, hepatitis B, foot-and-mouth virus, bovine viral diarrhea virus, feline calicivirus, and vaccinia virus [15, 17, 18], suggesting a potential of using PDAs as a colorimetric sensor for coronavirus detection [19–21]. To the best of our knowledge, no report has been published that describes a PDA-based colorimetric sensor to detect SARS-CoV-2.

In this study, a PDA-based flexible biosensor was developed for detecting the S protein of SARS-CoV-2, resulting in biosensors for SARS-CoV-2. The anti-N is an antibody protein of nucleocapsid (N) structural protein of SARS-CoV-2 that is responsible for the viral replication in host cells [22]. The anti-N protein is more sensitive to detect early COVID-19 infection in comparison to the antibody protein specific to the spike protein [23]. Therefore, the PDA-based flexible biosensor was prepared by electrospinning PDA nanofiber composite with the conjugation of SARS-CoV-2 anti-N protein. The carboxylic acid group (–COOH) in the PDAs was transformed into an open ester bond (–COO–) that provided a binding site for the anti-N. When the anti-N conjugated PDA nanofiber (PU-PDA-NHS-anti) was introduced to the spike protein of the SARS-CoV-2, the nanofibers demonstrated a colorimetric transition from blue to red after incubation and the intensity of the color of red was increased after 24 h of incubation. In a comparison with no color changes found in the non-functionalized PU-PDA fibers, the functionalized PU-PDA-NHS-anti fibers showed colorimetric responses to the S protein of SARS-CoV-2. The anti-N proteins in the PU-PDA-NHS-anti fibers probably interacted with the S protein which triggered the color change in the fiber. Because the PDA nanofibers were flexible and lightweight and did not require a power supply such as a battery when the colorimetric detection to S protein occurred, the PDA nanofibers could be used in developing wearable devices for detecting SARS-CoV-2. Wearable devices, which allow physiological signals to be continuously monitored, can be used in the early detection of asymptomatic and pre-symptomatic cases of COVID-19 [24]. Wearable devices such as facemasks and medical gowns using the PDA nanofiber composites can be potentially developed to monitor in real time the contamination of SARS-CoV-2.

To prepare the PU-PDA-NHS-anti nanofiber biosensor, at first, the 10,12-pentacosadiynoic acid (PCDA) monomer was chemically functionalized to PCDA-NHS (Supplementary Document). During this functionalization, the carboxylic acid groups (–COOH) of PCDAs were transformed into open ester bonds (–COO–). To confirm the functionalization, a Nicolet 6700 Fourier transform infrared spectroscopy (FTIR) spectrometer (Thermo Electron Corporation, Madison, WI, USA) was used to collect attenuated total reflection-FTIR spectra of the PCDA and PCDA-NHS powders. The FTIR spectra of PCDA-NHS powder had a peak at wavenumber 1723 cm^{-1} that corresponds to ester bond (–COO–). This peak was not found in PCDA powders. The PCDA powders showed a peak at wavenumber 1689 cm^{-1} corresponding to carboxylic acid (–COOH) stretching typical in PCDA [15] (Fig. 1).

Then, PCDA and PCDA-NHS powders and polyurethane (PU) matrix polymer were used to prepare PU-PDA-NHS fiber mats via electrospinning technique (Supplementary Document). Additionally, control samples of PU-PDA fiber mats were prepared by the procedures described in our previous report [11]. Both PU-PDA and PU-PDA-NHS fiber mats were blue (Fig. 2a). The fiber mats were peeled off from the aluminum foil as shown in Fig. 2b. Fibers were highly stretchable and curled up after peeling from the aluminum foil, suggesting good flexibility (Fig. 2c).

FTIR spectra of PU-PDA and PU-PDA-NHS fibers exhibited a similar trend as PCDA and PCDA-NHS powders. PU-PDA fibers showed a peak at wavenumber 1691 cm^{-1} (–COOH) that was not present in PU-PDA-NHS fibers. Instead, a new peak at wavenumber 1725 cm^{-1} (–COO–) was observed in PU-PDA-NHS fibers (Fig. 1). The results confirmed the esterification of PCDAs as a binding site for the anti-N protein [15, 18]. Finally, PU-PDA-NHS fiber mats were incubated with a solution containing 2 µg/mL anti-N protein for 48 h at 4 °C to prepare PU-PDA-NHS-anti fiber mats (Supplementary Document). No significant difference was found between the PU-PDA-NHS and PU-PDA-NHS-anti fibers when comparing the FTIR spectra (Fig. 1).

To confirm the anti-N conjugation occurring to the PU-PDA-NHS fibers, FTIR spectra were collected for PDA-NHS powders without PU. PCDA-NHS powders were photopolymerized and then UV irradiated at 254 nm for 3 min, resulting in PDA-NHS powders. The PDA-NHS powders were incubated with anti-N and FTIR spectra were taken before

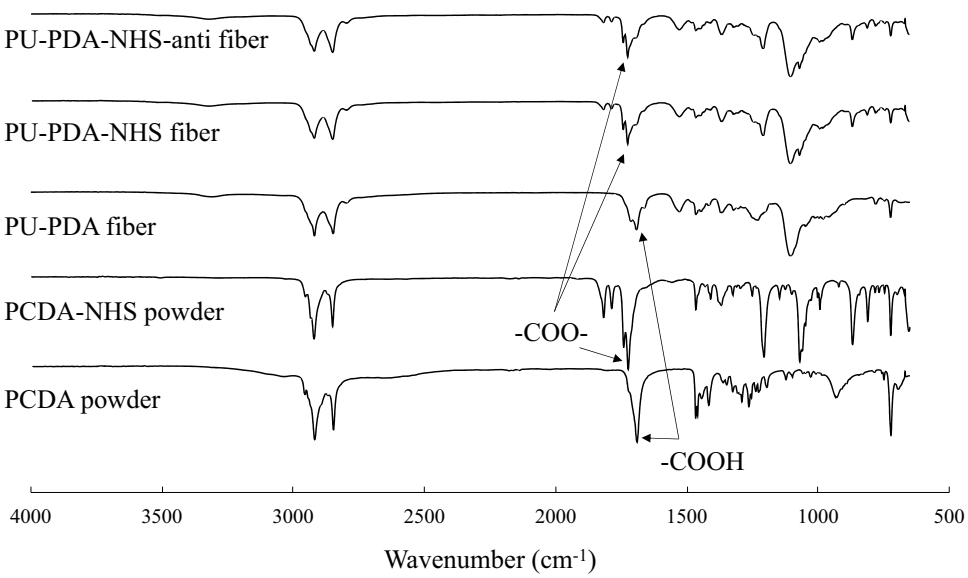

Fig. 1 FTIR spectra of PCDA powders and PDA fiber samples

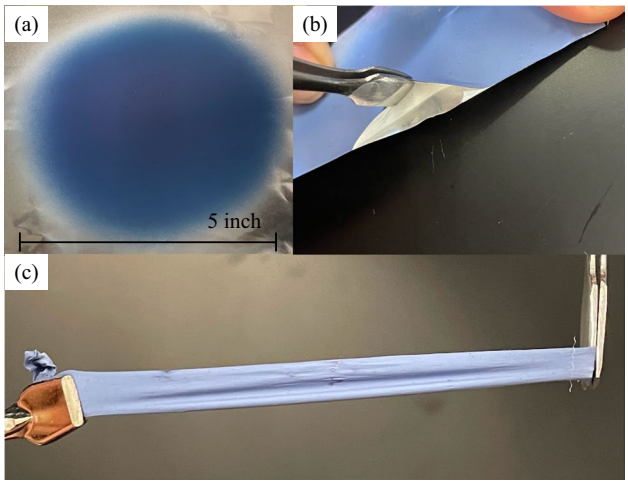

Fig. 2 Images of **a** PDA nanofiber mat, **b** fiber mat during peeling off the aluminum foil, and **c** demonstration of high stretchability

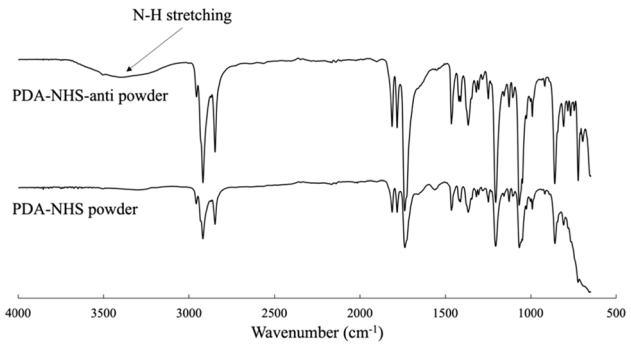

Fig. 3 FTIR spectra of PDA-NHS and PDA-NHS-anti powders

and after the incubation. The result showed a significant increase in the N–H stretching peak (3360 cm^{-1}) (Fig. 3 arrow marked), arising due to the presence of nitrogen (N) in anti-N protein composition. The presence of N–H stretching peak confirmed the successful anti-N conjugation with the PDA-NHS (Fig. 3).

After the preparation of PU-PDA-NHS-anti nanofiber biosensor, circular fiber samples were cut to fit inside a 48-well plate. The fiber samples were washed using sterile water and PBS before they were incubated in SARS-CoV-2 S protein (SinoBiological, Wayne, PA) solution (1 µg/mL) using a low attachment 48-well plate at room temperature. The S protein preparation method with the buffer solution concentration can be found in the Supplementary Document. The S protein solution was diluted using a dilution factor suggested by the manufacturer. All the results reported here were obtained using the dilution factor of 1:500 that determined the protein concentration was 1 µg/mL. Previous report from our lab confirmed that PDA nanofibers do not change color at temperature less than 60 °C [10], so temperature during testing condition did not affect the colorimetric or morphological properties of the PDA nanofibers. Control samples of PU-PDA and PU-PDA-NHS fibers were also incubated with S protein solution. Morphological analysis of the fibers was conducted before and after the S protein incubation using scanning electron microscopic (SEM) images. A JEOL JSM-6500 field emission scanning electron microscope was used to collect SEM images. The results showed that PU-PDA fibers had a scale-like structure on the fiber surface which confirmed the attachment of PDAs on the PU fibers [11, 12] (Fig. 4). PU-PDA-NHS fibers had a similar morphology on the surface (Fig. 4). The PU-PDA-NHS-anti fibers had a similar structure but had some dot-like structures on the surface, which might be the anti-N proteins because this fiber was incubated for 48 h in

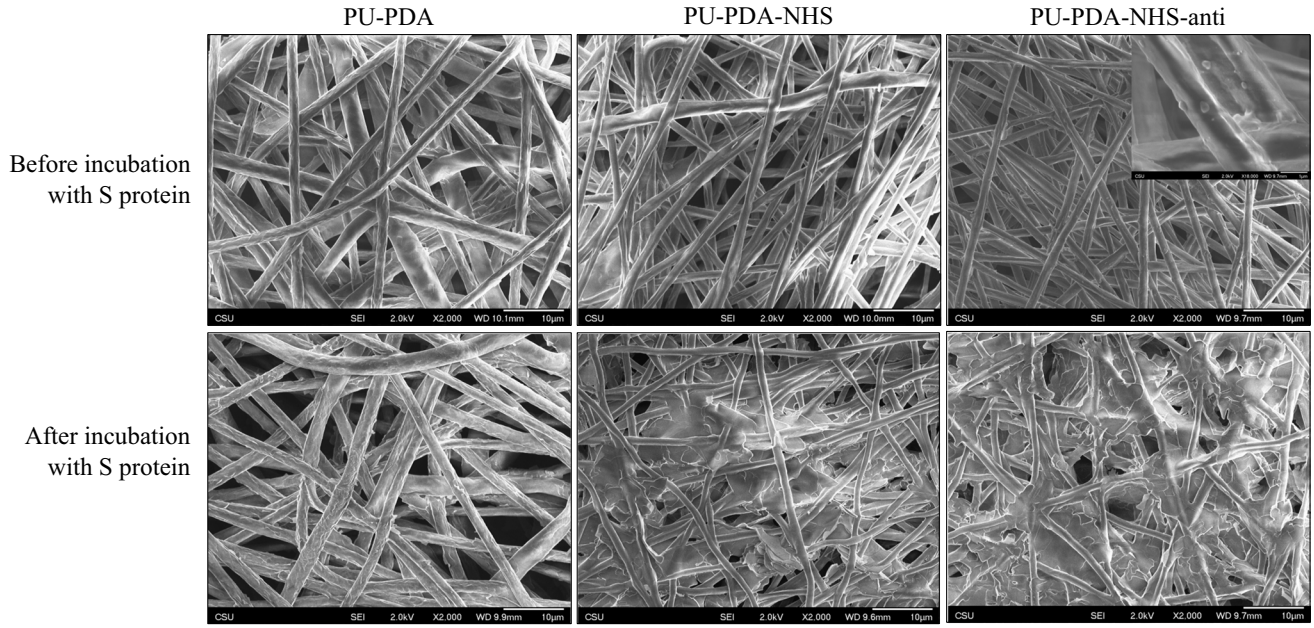

Fig. 4 SEM images PDA fibers before and after incubation with S protein

the anti-N protein solution (Fig. 4, inset). The size of these dot-like structures varied from 50 to 700 nm, indicating different degrees of coagulation of antibody protein on the fiber surface. After 24 h of incubation with S protein, the PU-PDA fiber morphology remained the same, suggesting no chemical reaction between the fiber and S protein (Fig. 4). In comparison, the PU-PDA-NHS and PU-PDA-NHS-anti fibers showed a very rough surface after incubation with S protein (Fig. 4). Larger scale-like structures were observed in the fibers. The results indicated the topographical changes in the fiber morphology might be due to the interaction between the fibers (PU-PDA-NHS and PU-PDA-NHS-anti) and S protein.

From the SEM images, fiber diameters were measured using the ImageJ software. Ten fiber samples from each category were analyzed for fiber diameter analysis before and after incubation with S protein. The average diameter of PU-PDA nanofibers was 1700 nm. The PU-PDA-NHS and PU-PDA-NHS-anti nanofibers had average diameters of 1200 and 1300 nm respectively. The reduction of diameter in PU-PDA-NHS and PU-PDA-NHS-anti fibers was likely due to the addition of functionalized PCDA-NHS in the electrospinning solution. While electrospinning, the fibers were deposited randomly on the collector plate due to the high electrostatic force. So, the size of the nanofibers was not same for all the fibers, but rather had a range of diameters as shown in Fig. 5. The variation in diameter was not drastic compared to the previously reported PDA nanofibers prepared via electrospinning [11, 13, 25]. To evaluate statistically significant differences in the fiber diameters, analysis

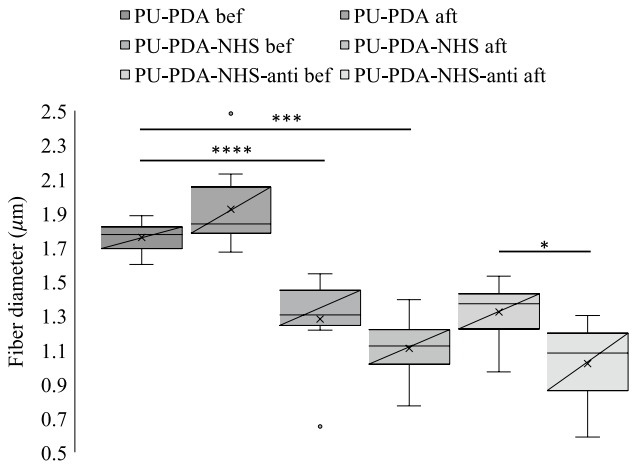

Fig. 5 PDA fiber diameter before and after incubation with S protein. ANOVA and HSD were performed for statistical analysis (*, ***, and **** indicate $p \leq 0.05$, $p \leq 0.001$, and $p \leq 0.0001$)

of variance (ANOVA) and Tukey's honest significant difference (HSD) tests were performed. The results (Fig. 5) indicated that there was no significant difference between PU-PDA fibers before and after S protein incubation, which is in good agreement with the morphological observation of the fibers and indicated that the S protein did not react with the PU-PDA fibers. The diameters of the PU-PDA-NHS and PU-PDA-NHS-anti fibers were reduced after S protein incubation, which was likely due to the interaction between PDA fibers and S proteins. However, the diameter reduction in PU-PDA-NHS fiber after S protein incubation was not

statistically significant. Fiber morphology and fiber diameter may change due to changes in electrospinning parameters [26], and addition of surfactants, chemicals, and drug molecules [27], as well as external stimuli [28]. Previous studies reported a diameter increase and a scale-like morphological change in the PU-PDA fibers in comparison with pristine PU fibers [11]. When the PDAs were modified to prepare PU-PDA-NHS and PU-PDA-NHS-anti fibers, the scale-like structure was also observed (Fig. 4). Then, after the fibers were incubated with S protein, the scales on fiber surface were disrupted as shown in Fig. 4. A hypothesis was that the changes in fiber surface morphology were due to the interaction between antibody conjugated PDA-NHS and S protein. Figure 4 shows no changes found in the PU-PDA fiber after incubation with S protein. It was likely because there was no interaction with the S protein due to the absence of PDA-NHS or PDA-NHS-anti. The nature and dynamics of the interaction between PDA-NHS-anti molecules in the fibers with S protein of SARS-CoV-2 needs further experimental analysis.

When the PU-PDA-NHS-anti fiber was incubated with S protein (1 µg/mL) at room temperature, the fiber started changing color from blue to red after 4 h of incubation. The color of red became bright after 24 h of incubation (Fig. 6a). In addition, PU-PDA and PU-PDA-NHS fibers were incubated with the S protein. No color change was observed in PU-PDA fibers as expected, which was in good agreement with the morphological observation and fiber diameter analysis. Furthermore, a significant color change was observed in PU-PDA-NHS fiber after 24 h of incubation with S protein (Fig. 6a). That was because the PU-PDA-NHS fiber had open ester groups (–COO–) on macromolecules, and hence some S proteins might have been able to conjugate to the PU-PDA-NHS fiber, resulting in a color change. Additionally, all the fibers were incubated with the buffer solution that was used to prepare the S protein solution and no color change was observed. The buffer solution was composed of 0.1% bovine serum albumin (BSA) protein in wash buffer (Supplementary Document). The PDA fibers did not change color when they were incubated with buffer solution, thus signifying a specific detection of S protein.

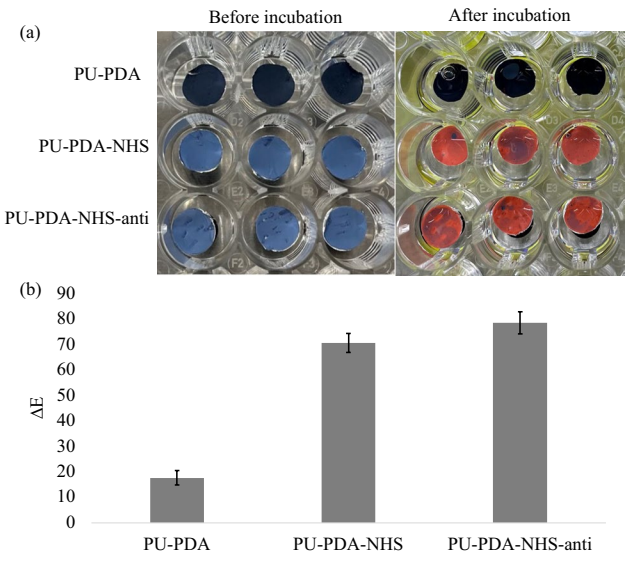

Fig. 6 **a** Photographs of PDA fibers before and after 24 h of incubation with S protein, **b** ΔE values of PDA fibers

The color change in the fibers was quantified using CIE (International Commission of Illumination) color space coordinates that include the values of L*, a*, and b* representing lightness, color position between green and red, and color position between yellow and blue respectively [29]. Photographs of PDA fibers were taken before and after 24 h of incubation with S protein (Fig. 6). CIE L*a*b* values were obtained from the photograph using Digital Color Meter application (Apple Inc.). Twenty values of L*, a*, and b* were collected for each fiber on the photographs. Ten values were for samples before incubation and 10 values were for after incubation. The color change of the fibers was quantified by calculating the ΔE values using Eq. (1).

$$\Delta E = \sqrt{(\Delta L)^2 + (\Delta a)^2 + (\Delta b)^2} \quad (1)$$

where ΔL, Δa, and Δb are the differences in brightness, redness, and yellowness of the fibers before and after the incubation with S protein [29], respectively. The ΔE values are shown in Fig. 6b. The ΔE for PU-PDA was 17.61, which is very low compared to the ΔE of PU-PDA-NHS (70.52) and PU-PDA-NHS-anti (78.49) fibers. The higher ΔE of PU-PDA-NHS and PU-PDA-NHS-anti fibers confirmed a distinguishable color change in the fibers after incubation with S protein. Additionally, it was observed that the difference in the ΔE between PU-PDA-NHS and PU-PDA-NHS-anti was very minimum, suggesting that the antibody functionalization may not be necessary for S protein detection. The removal of antibody conjugation can offer cost reduction in biosensor preparation; however, because the color change in PU-PDA-NHS fiber was not proven specifically due to the open ester bond, more control experiments need to be conducted in the future to fully understand the specificity of the fiber.

The average L*a*b* of the fibers before and after incubation with S protein were measured. A negative a* value represents green region but positive a* represents red, and a negative b* indicates blue whereas a positive b* indicates yellowness [30]. b* of all fibers were negative before S protein incubation, meaning the fibers were blue. However, after the incubation, only PU-PDA fiber's b* remained negative (− 5.749) which indicated the fiber color remained blue after S protein incubation. On the other hand, a* values of PU-PDA-NHS (44.341) and PU-PDA-NHS-anti (48.614)

became positive after S protein incubation, indicating the color of these fibers shifted to red.

The vivid blue to the red transformation of the PU-PDA-NHS-anti fiber suggested an interaction between the S protein and the anti-N protein that might have been responded by a perturbation in the electron cloud of the PDAs and resulted in a color change. The nature of this protein–protein interaction between anti-N and S proteins will be investigated in the future. The initial indication of this protein–protein interaction can help to prepare targeted therapeutics and efficient biosensors that can effectively sense and inactivate the SARS-CoV-2 in the respiratory cells. The preliminary results that were illustrated here have demonstrated that the antibody conjugated PDA nanofibers have the potential in creating wearable devices and personal protective equipment such as face masks and medical gowns for real-time detecting and monitoring SARS-CoV-2 contamination and contraction on a daily basis as well as in a healthcare setting. Further investigation will focus on sensitivity, selectivity, and biosafety of PDA's colorimetric responses to S protein, which are critical in proof-of-concept of using PDAs in SARS-CoV-2 detection techniques. Additional studies such as comparability and durability of the flexible PDA nanofibers should be considered with the textile materials commonly used in personal protective equipment such as facemasks and medical gowns. A viral load model was described by Soto et al. (2021), where a 4-h timeframe provided a sufficient threshold number of virus captured by a functionalized face mask to perform analytical analysis [31]. The PDA nanofiber biosensor described in this work exhibited a color change after 4 h of incubation with the S protein of SARS-CoV-2, which was consistent with the timeframe reported by Soto et al. (2021) [31]. The 4-h timeframe is a good indication of mask wearing base requirement for an effective sensing of the virus via a mask protection. Future work would require a detection study with live SARS-CoV-2 as well as an optimization study of electrospinning parameters and antibody concentration in the fiber to improve the sensitivity of the PDA nanofibers.

PDA nanofibers were obtained via chemical functionalization of PCDA monomer and electrospinning, resulting in a binding site for a receptor molecule—nucleocapsid antibody (anti-N) protein of SARS-CoV-2. The anti-N protein was attached to the functionalized PDA fibers via conjugation, resulting in PU-PDA-NHS-anti fibers. The PU-PDA-NHS-anti fibers showed a colorimetric transition from blue-to-red when interacting with S protein of SARS-CoV-2 at room temperature, suggesting it was a colorimetric detection of SARS-CoV-2. The results demonstrated the potential of using PDA nanofibers in creating a flexible, lightweight, no-battery, and colorimetric biosensor. The PDA biosensors can be used in developing wearable devices and personal protective equipment such as face masks and medical gowns, providing real-time detection to COVID-19 contraction and hence timely medical decisions to improve public health in pandemics. In addition, the flexible PDA biosensors can be used in hygiene products, food processing, and food packaging, providing real-time detection via colorimetric indication. These smart products will empower individuals in the decision-making process and improve health and well-being.

Supplementary Information The online version contains supplementary material available at https://doi.org/10.1007/s44164-022-00022-z.

Acknowledgements The authors would like to thank the Analytical Resources Core (ARC, Research Resource ID: SCR_021758) at Colorado State University, Fort Collins, for helping in taking SEM images of the fibers.

Funding The work was funded by the Student Research Support Grant provided by the American Association of Textile Chemists and Colorists (AATCC) and financial contributions from the Office of Vice President for Research (OVPR) at Colorado State University, Fort Collins, USA.

Declarations

Conflict of interest The authors declare no competing interests.

References

1. Hoffmann M, Kleine-Weber H, Schroeder S, Krüger N, Herrler T, Erichsen S, Schiergens TS, Herrler G, Wu N-H, Nitsche A, Müller MA, Drosten C, Pöhlmann S. SARS-CoV-2 cell entry depends on ACE2 and TMPRSS2 and is blocked by a clinically proven protease inhibitor. Cell. 2020;181(2):271–80. https://doi.org/10.1016/j.cell.2020.02.052.
2. Zhu N, Zhang D, Wang W, Li X, Yang B, Song J, Zhao X, Huang B, Shi W, Lu R, Niu P, Zhan F, Ma X, Wang D, Xu W, Wu G, Gao GF, Tan W. A novel coronavirus from patients with pneumonia in China, 2019. N Engl J Med. 2020;382:727–33. https://doi.org/10.1056/NEJMoa2001017.
3. Coronavirus Disease 2019 (COVID-19) Situation Report - 51. World Health Organization. 2020. https://www.who.int/docs/default-source/coronaviruse/situation-reports/20200311-sitrep-51-covid-19.pdf?sfvrsn=1ba62e57_10. Accessed 11 March 2020.
4. Weekly Operational Update on COVID-19, Issue No. 80. World Health Organization. 2021. https://www.who.int/publications/m/item/weekly-operational-update-on-covid-19---15-november-2021. Accessed 16 Nov 2021.
5. Ashour HM, Elkhatib WF, Rahman MM, Elshabrawy HA. Insights into the recent 2019 novel coronavirus (SARS-CoV-2) in light of past human coronavirus outbreaks. Pathogens. 2020;9(3):186–201. https://doi.org/10.3390/pathogens9030186.
6. Zhou P, Yang X-L, Wang X-G, Hu B, Zhang W, Si H-R, Zhu Y, Li B, Huang C-L, Chen H-D, Chen J, Luo Y, Guo H, Jiang R-D, Liu M-Q, Chen Y, Shen X-R, Wang X, Zheng X-S, Zhao K, Chen Q-J, Deng F, Liu L-L, Yan B, Zhan F-X, Wang Y-Y, Xiao G-F, Shi Z-L. A pneumonia outbreak associated with a new coronavirus of probable bat origin. Nature. 2020;579:270–3. https://doi.org/10.1038/s41586-020-2012-7.

7. Suman R, Javaid M, Haleem A, Vaishya R, Bahl S, Nandan D. Sustainability of coronavirus on different surfaces. J Clin Exp Hepatol. 2020;10(4):386–90. https://doi.org/10.1016/j.jceh.2020.04.020.
8. Lai C-C, Wang C-Y, Ko W-C, Hsueh P-R. In vitro diagnostics of coronavirus disease 2019: Technologies and application. J Microbiol Immunol Infect. 2021;54(2):164–74. https://doi.org/10.1016/j.jmii.2020.05.016.
9. Talebian S, Wallace GG, Schroeder A, Stellacci F, Conde J. Nanotechnology-based disinfectants and sensors for SARS-CoV-2. Nat Nanotechnol. 2020;15:618–21. https://doi.org/10.1038/s41565-020-0751-0.
10. Alam AKMM, Yapor J, Reynolds MM, Li YV. Study of polydiacetylene-poly (ethylene oxide) electrospun fibers used as biosensors. Materials. 2016;9(3):1–13. https://doi.org/10.3390/ma9030202.
11 Bhattacharjee A, Clark R, Gentry-Weeks C, Li YV. A novel receptor-free polydiacetylene nanofiber biosensor for detecting *E. coli* via colorimetric changes. Mater Adv. 2020;1(9):3387–97. https://doi.org/10.1039/D0MA00619J.
12. Hassan F, Gentry-Weeks C, Reynolds M, Li YV. Study on microstructure and mechanical properties of polydiacetylene composite biosensors. J Appl Polym Sci. 2019;136(34):47877. https://doi.org/10.1002/app.47877.
13. Yapor JP, Alharby A, Gentry-Weeks C, Reynolds MM, Alam AKMM, Li YV. Polydiacetylene nanofiber composites as a colorimetric sensor responding to *Escherichia coli* and pH. ACS Omega. 2017;2(10):7334–42. https://doi.org/10.1021/acsomega.7b01136.
14. Bhattacharjee A, Clark R, Gentry-Weeks C, Li YV. Study of bacterial components activating a colorimetric transition in bacteria-detecting nanofiber wound dressing applications. International Textile and Apparel Association Annual Conference Proceedings. 2020;77(1). https://doi.org/10.31274/itaa.12123.
15. Son SU, Seo SB, Jang S, Choi J, Lim J-W, Lee DK, Kim H, Seo S, Kang T, Jung J, Lim E-K. Naked-eye detection of pandemic influenza A (pH1N1) virus by polydiacetylene (pda)-based paper sensor as a point-of-care diagnostic platform. Sensors Actuators B Chem. 2019;291:257–65. https://doi.org/10.1016/j.snb.2019.04.081.
16. Charych DH, Nagy JO, Spevak W, Bednarski M. Direct colorimetric detection of a receptor-ligand interaction by a polymerized bilayer assembly. Science. 1993;261(5121):585–8. https://doi.org/10.1126/science.8342021.
17. Jiang L, Luo J, Dong W, Wang C, Jin W, Xia Y, Wang H, Ding H, Jiang L, He H. Development and evaluation of a polydiacetylene based biosensor for the detection of H5 influenza virus. J Virol Methods. 2015;219:38–45. https://doi.org/10.1016/j.jviromet.2015.03.013.
18. Song S, Ha K, Guk K, Hwang S-G, Choi JM, Kang T, Bae P, Jung J, Lim E-K. Colorimetric detection of influenza A (H1N1) virus by a peptide-functionalized polydiacetylene (PEP-PDA) nanosensor. RSC Adv. 2016;6:48566–70. https://doi.org/10.1039/C6RA06689E.
19. Qian X, Städler B. Polydiacetylene-based biosensors for the detection of viruses and related biomolecules. Adv Funct Mater. 2020;30(49):2004605. https://doi.org/10.1002/adfm.202004605.
20. Bukkitgar SD, Shetti NP, Aminabhavi TM. Electrochemical investigations for COVID-19 detection-a comparison with other viral detection methods. Chem Eng J. 2021;420(2):127575. https://doi.org/10.1016/j.cej.2020.127575.
21. Tymm C, Zhou J, Tadimety A, Burklund A, Zhang JXJ. Scalable COVID-19 detection enabled by lab-on-chip biosensors. Cell Mol Bioeng. 2020;13:313–29. https://doi.org/10.1007/s12195-020-00642-z.
22. Troyano-Hernáez P, Reinosa R, Holguín Á. Evolution of SARS-CoV-2 envelope, membrane, nucleocapsid, and spike structural proteins from the beginning of the pandemic to September 2020: a global and regional approach by epidemiological week. Viruses. 2021;13(2):243. https://doi.org/10.3390/v13020243.
23. Burbelo PD, Riedo FX, Morishima C, Rawlings S, Smith D, Das S, Strich JR, Chertow DS, Davey RT Jr, Cohen JI. Sensitivity in detection of antibodies to nucleocapsid and spike proteins of severe acute respiratory syndrome coronavirus 2 in patients with coronavirus disease 2019. J Infect Dis. 2020;222(2):206–13. https://doi.org/10.1093/infdis/jiaa273.
24. Ates HC, Yetisen AK, Güder F, Dincer C. Wearable devices for the detection of COVID-19. Nat Electron. 2021;4:13–4. https://doi.org/10.1038/s41928-020-00533-1.
25. Kim JH, Lee JS. Development of polydiacetylene embedded polyurethane nanocomposites as a mask for sensing and filtering fine dust. Fibers Polym. 2021;22:489–97. https://doi.org/10.1007/s12221-021-0187-7.
26. Bhardwaj N, Kundu SC. Electrospinning: a fascinating fiber fabrication technique. Biotechnol Adv. 2010;28(3):325–47. https://doi.org/10.1016/j.biotechadv.2010.01.004.
27. Zeng J, Xu X, Chen X, Liang Q, Bian X, Yang L, Jing X. Biodegradable electrospun fibers for drug delivery. J Control Release. 2003;92(3):227–31. https://doi.org/10.1016/S0168-3659(03)00372-9.
28. Aussawasathien D, Dong JH, Dai L. Electrospun polymer nanofiber sensors. Synth Met. 2005;154(1–3):37–40. https://doi.org/10.1016/j.synthmet.2005.07.018.
29. Arafat MT, Mahmud MM, Wong SY, Li X. PVA/PAA based electrospun nanofibers with pH-responsive color change using bromothymol blue and on-demand ciprofloxacin release properties. J Drug Deliv Sci Technol. 2021;61:102297. https://doi.org/10.1016/j.jddst.2020.102297.
30. Agarwal A, Raheja A, Natarajan TS, Chandra TS. Development of universal pH sensing electrospun nanofibers. Sensors Actuators B Chem. 2012;161(1):1097–101. https://doi.org/10.1016/j.snb.2011.12.027.
31. Soto F, Ozen MO, Guimarães CF, Wang J, Hokanson K, Ahmed R, Reis RL, Paulmurugan R, Demirci U. Wearable collector for noninvasive sampling of SARS-CoV-2 from exhaled breath for rapid detection. ACS Appl Mater Interfaces. 2021;13(35):41445–53. https://doi.org/10.1021/acsami.1c09309.